Photoelectron-spectroscopy study of amorphous a-CN_x:H

A. Mansour and D. Ugolini*
Institut für Physik der Universität Basel, Klingelbergstrasse 82, CH-4056 Basel, Switzerland
(Received 26 May 1992)

We report *in situ* x-ray photoemission, ultraviolet photoemission (UPS), and electron-energy-loss photoelectron-spectroscopy studies of the electronic structure of nitrogen-containing amorphous hydrogenated carbon (a-CN_x:H). Films with different nitrogen concentrations are prepared by the ion-beam-deposition technique. The photoemission measurements do not reveal a shift in the Fermi level with respect to the top of the valence band, as would be expected from an n-type nitrogen-doping mechanism proceeding via substitution. The C 1s core-level shifts observed as a function of nitrogen content are identified as chemical in nature, and the variation in line shape and peak position is explained in terms of a two-phase superposition model. A simple model fit to the He I UPS valence-band spectra reveals the effects of nitrogen on the spectral shape. It illustrates, in particular, the sensitivity of the partial p-π density of states (DOS) to the presence of nitrogen, and confirms the role played by the π bonds in controlling the electronic structure of a-C:H. The observed increases in area and width of the p-π DOS with increasing nitrogen content are in line with an existing model which favors a defect density increase and a size increase of the graphitelike islands formed by the clustering of π states in aromatic rings.

I. INTRODUCTION

There has been considerable interest in the past few years in hydrogenated amorphous carbon films (a-C:H) due to a large extent to their outstanding "diamondlike carbon" properties (high hardness, high transparency, high resistivity, chemical inertness), and their potential use in microelectronics, optics, and wear resistance.[1–3] In contrast, less attention has been devoted to the study of their semiconducting properties; Meyerson and Smith[4] have demonstrated the n- and p-type doping of these materials.

The first report of the use of nitrogen for doping amorphous carbon films was made in 1982 by Jones and Stewart.[5] However, to date, issues related to nitrogen doping efficiency and the doping mechanism are still controversial. In view of the low doping efficiency and the small observed changes in activation energy as a function of dopant concentration, Jones and Stewart[5] suggested that true substitutional doping was not occurring. They argued that the enhancement in the electrical conductivity after doping is not due to a shift of the Fermi level E_F with respect to the valence states, but rather to a modification of the density of localized states in a way that moves the conduction-band minimum closer to E_F. Amir and Kalish[6] interpreted their thermopower measurements in the mV/K range for films with low nitrogen content (<1 at. %) as supporting a mechanism of conductivity in the valence-band tail. A hopping conductivity around the Fermi level was inferred from their thermopower results in the μV/K regime for films of higher nitrogen concentrations. Such a doping mechanism would be in agreement with the model by Robertson and O'Reilly[7,8] which favors a substitutional but strongly compensated doping. This autocompensation mechanism is supported by the similar doping efficiency of nitrogen and phosphorus in a-C:H,[5] as opposed to the exceedingly inefficient nitrogen doping in a-Si:H as compared to phosphorus.[9] The influence of nitrogen incorporation on the structural and optical properties of nitrogenated amorphous carbon films (a-CN_x:H) films was studied by Han and Feldman,[10] and by Kaufman and co-workers.[11] The latter reported a hard a-CN_x:H which retained the basic structure and properties of undoped hard carbon. The former attributed the dominant NH_2 modes in the infrared absorption spectra to that of a polymeric structure.

Lin and co-workers[12] reported on the role of nitrogen as a passivator of dangling bonds, a role similar to the one played by hydrogen in hydrogenated amorphous silicon. They inferred from their electrical measurements a reduction in the density of defect states on going from a-C:H to a-CN_x-H, in good agreement with their electron-spin resonance (ESR) measurements. They concluded that such a decrease would correspond in effect to an increase in structural order with increasing nitrogen concentration. On the other hand, Amir and Kalish[6] suggested that the high level of electron paramagnetic resonance (EPR) active centers deduced from their EPR measurements, and the slight rise of the spin density with the addition of nitrogen may support the arguments of Robertson and O'Reilly[7,8] that doping is likely to be accompanied by the formation of additional dangling-bond defects. The presence of these additional dangling-bond defects would result, through an autocompensation process, in the low doping efficiency observed in these materials.

It may then seem that underlying all these properties and resting at the center of our understanding of these modified materials is the question of their electronic structure. One clue to understanding the mechanism responsible for doping may result from an accurate and detailed characterization of the density of states of the valence band. How the electronic states near the valence-

and conduction-band edges and in the gap region are modified largely determine the electrical, optical, and vibrational properties of these materials. a-C:H consists of clusters of threefold coordinated sp^2 (trigonal) carbon (graphitelike) embedded in a fourfold coordinate sp^3 (tetrahedral) bonded matrix (diamondlike). The graphitelike atoms at sp^2 sites form clusters with three localized sp^2 hybrid states per atom (σ bonds), while the π states remain delocalized and form weaker bonds to neighboring sites.[7,8] It is the graphitelike π bonds at sp^2 sites that are responsible for controlling the electronic structure of a-C:H due, to a large extent, to the weak bonding character and their delocalized nature: these states will lie closest to the Fermi level and will form both the valence- and conduction-band edge states.[7,8] The study of the π electronic structure becomes then essential in order to derive information on the electronic properties of a-CN_x:H.

In order to address this question, we report in this paper x-ray photoemission (XPS), ultraviolet photoemission (UPS), and electron-energy-loss (EELS) spectroscopic investigations of nitrogen-containing hydrogenated amorphous carbon films prepared by ion-beam deposition (BD). The samples have been prepared *in situ* and transferred from the preparation site to the measuring chamber under UHV conditions so that the inherent nature of the chemical reaction of nitrogen with the hydrogenated amorphous carbon host is preserved.

II. EXPERIMENT

The a-C:H and a-CN_x:H films used in this study have been prepared by the IBD technique using a Kaufman-type source.[13] The source is fitted to the preparation chamber of a combined UPS/XPS/AES/EELS (where AES denotes Auger electron spectroscopy) spectrometer equipped with a hemispherical Leybold-Heraeus EA10/100 electron-energy analyzer. The operating principle of the ion source has been described elsewhere.[14] The ion source was operated at 400-eV ion energy with pure methane for a-C:H and a mixture of methane and nitrogen for a-CN_x:H. The deposition chamber was pumped by a 220 l/s turbomolecular ion pump, with a base pressure of 1×10^{-9} mbar, while the total pressure was maintained at about 2×10^{-3} mbar throughout deposition. The nitrogen level was varied by increasing the nitrogen content in the gas mixture during film deposition, keeping the total pressure constant, and the total gas flow rate, controlled by two BROOKS regulators, constant at values between 7.2 and 7.5 SCCM, where SCCM denotes cubic centimeter per minute at STP.

The films were deposited on a gold substrate held at room temperature throughout deposition. Prior to deposition, the substrate was cleaned by repeated 5-keV-Ar^+ ions sputtering-annealing cycles. The sputter cleaning-annealing procedure was applied until no contaminants such as oxygen or carbon could be detected by widescan XPS core-level analysis. No concentration of elements other than carbon (in the case of a-C:H) and nitrogen and carbon (in the case of a-CN_x:H) could be detected in the films following deposition; specifically, no oxygen contamination was observed within the detection limits of the technique.

The choice of gold as a substrate was dictated by the fact that Au does not react chemically with the a-C:H overlayer.[15] This is important because a passive interface prevents the formation of strong covalent bonds characteristic of a carbidic interface phase which may influence the photoelectron spectroscopy measurements through additional binding-energy shifts of the core levels as well as valence-band spectra. Another incentive for choosing a metallic substrate such as Au is to avoid charging effects that can severely influence photoelectron-spectroscopy measurements of highly insulating materials. Typically, charging arises from the establishment of a positive charge within the surface region of the insulating film from which the photoelectron originated, since a charge compensating current cannot pass from the substrate to the sample surface. The effect of this charging on the recorded photoelectron spectra is abnormally large positive binding-energy shifts. An appropriate film thickness is chosen in a way as to prevent the formation of the positive charge by the injection of photoelectrons from the conducting substrate into the insulating film. We determine this thickness by monitoring the gradual disappearance of the photoelectron signal originating from the substrate. That corresponds to the Au Fermi edge in the UPS valence-band spectra.

The UPS spectra are measured with a resonance lamp using either He I ($h\nu=21.2$ eV) or He II ($h\nu=40.8$ eV) resonance lines. The spectrometer is operated in the constant retardation ratio mode. The energy resolution is of the order of 0.1 and 0.2 eV for He I and He II radiation, respectively. The XPS core-level data are measured with Mg Kα excitation ($h\nu=1253.6$ eV) and spectrometer pass energy of 50 eV (FAT mode). The energy resolution in this case is of the order of 1.0 eV. Core-level binding-energy shifts are measured within 0.1-eV accuracy. The binding energy of the Au $4f_{7/2}$ core level is taken to be 84.0 eV for energy calibration. The EELS spectra are recorded using a 500-eV electron gun, with the spectrometer operated with pass energy of 10 eV, leading to an overall energy resolution of about 0.5 eV. The base pressure in the spectrometer is 1.0×10^{-9} mbar.

III. RESULTS AND DISCUSSION

A. The C 1s and N 1s core levels

The nitrogen content (x) incorporated in the a-CN_x:H films can be obtained from the ratio of integrated net intensities of the N 1s to C 1s lines, corrected by the corresponding photoionization cross sections as given by Scofield.[16] Figure 1(a) shows the nitrogen concentration in the films as a function of the relative nitrogen concentration, $N_2/(N_2+CH_4)$, in the gas phase. The photoelectron spectra have been obtained for deposition times of 3 min for a-C:H, and 7.5, 8.0, and 8.5 min for a-CN_x:H with $x=0.03$, 0.07, and 0.1, respectively [Fig. 1(b)]. These are the times necessary to obtain the optimum thickness required for photoelectron measurements, which we estimate to be about 70 Å. At this thickness,

which has been determined by monitoring for the disappearance of the Au Fermi edge, the layer is thick enough for all the photoelectrons to originate from the film itself without being influenced by the interface region underneath. It is also thin enough for charging effects to be ignored.

The longer deposition time required to achieve the same film thickness at higher nitrogen concentration reflects a decreasing deposition rate from the competing sputtering effect of nitrogen. Under the constant total pressure experimental conditions, the increasingly lower hydrocarbon to nitrogen ratio is likely to result in a lower deposition rate as well. Nitrogen concentrations up to $x = 0.1$ can be incorporated in the films; however, higher nitrogen content of the required thickness for the photoelectron measurements could not be achieved.

Figure 2 shows the XPS C 1s and N 1s core-level spectra of a series of a-CN_x:H films with various nitrogen concentrations. Here the binding energies refer to the Fermi level E_F. As the nitrogen concentration increases, the C 1s peak shifts towards higher binding energy, and a broadening and asymmetry in the line shape are observed. On the other hand, the binding energy and the linewidth of the N 1s core level remain constant for the entire range of nitrogen concentrations. All binding-energy values fall within the range of 399.5 ± 0.1 eV, and the full width at half maximum (FWHM) of the core-level spectra remains constant at 2.4 eV.

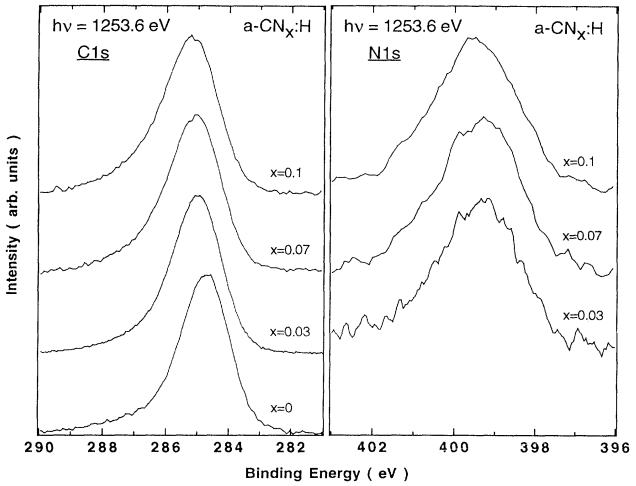

FIG. 2. XPS C 1s and N 1s core-level spectra in a-CN_x:H for selected nitrogen concentrations x measured with Mg $K\alpha$ radiation.

Binding energies (relative to E_F) of the C 1s core levels and linewidths are plotted as a function of the nitrogen content (x) in Fig. 3. The binding energy increases monotonically from 284.8 eV in a-C:H up to 285.2 eV in a-CN_x:H ($x = 0.1$). This increase is more rapid for small x values ($0 < x < 0.03$) than for concentration larger than 0.03: a 0.3-eV shift for x in the range of 0 to 0.03, as compared to a 0.1-eV shift as the nitrogen content in-

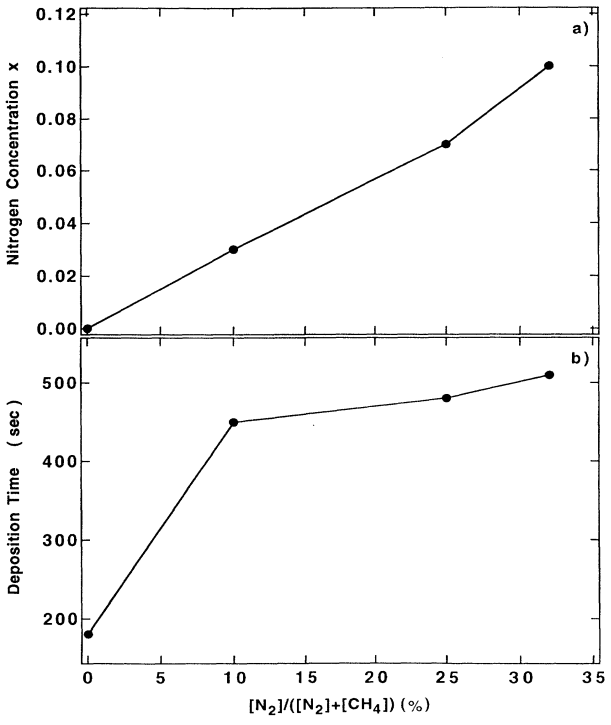

FIG. 1. (a) Nitrogen concentration x in a-CN_x:H as estimated from the intensity ratio of the N 1s to C 1s core-level lines as a function of the N_2 gas ratio $N_2/(N_2+CH_4)$. (b) Deposition time required for photoelectron measurements as explained in the text as a function of the N_2 gas ratio $N_2/(N_2+CH_4)$.

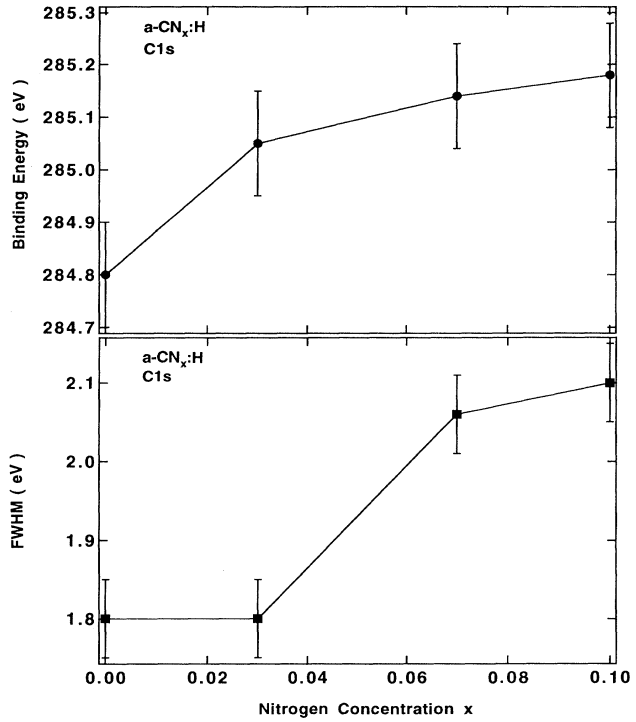

FIG. 3. Peak binding energy (relative to E_F) and FWHM of the C 1s core level of a-CN_x:H as a function of the nitrogen concentration x.

creases from 0.03 to 0.1. On the other hand, the initial 0.3-eV binding energy increase is not accompanied by an increase of the linewidth, as opposed to the gradual linewidth increase from a FWHM value of 1.80 eV for $0<x<0.03$ to a maximum value of 2.10 eV for $x=0.1$. A line superposition of a-C:H and a-CN_x:H for $x>0.03$ reveals an asymmetric broadening of the C 1s line shape in a-CN_x:H with a distinct tailing towards higher binding energy.

The observed shifts of the C 1s binding energy as a function of the nitrogen content (x) cannot be attributed to charging, since special care has been taken in choosing the optimum thickness for photoelectron measurements as discussed above. In fact, whereas the onset of charging is observed at higher thicknesses of a-C:H films, indicative of their insulating nature, such an effect is absent in the case of nitrogen-containing films (i.e., no binding-energy shifts are observed for thicker films). This absence of charging is correlated with an increase of the electrical conductivity of the nitrogen-containing films.[5,6,10]

The dependence of the C 1s binding energy on the nitrogen content can be understood in terms of either chemical shifts of the XPS line or shifts "other than chemical" in nature. In the latter, an upward shift of the Fermi level E_F leads to an increase in binding energies relative to E_F. As direct consequence of a Fermi-level shift, all core-level binding energies (measured relative to E_F) should be affected in the same way. But in view of the fact that the N 1s binding energy remains constant as x increases, the shifts of the C 1s XPS lines cannot be explained in terms of shifts of E_F. Instead they are to be considered a result of chemical shifts on charge transfer: The incorporation of nitrogen in the a-C:H matrix induces a charge transfer from the less electronegative C (2.5) (Ref. 17) atoms to the more electronegative N (3.0) (Ref. 17) atoms. This decrease in the electron density on the C atoms results in a shift of all C core levels towards higher binding energies, as more homopolar C–C bonds are replaced by heteropolar C–N bonds. Small chemical shifts connected with induction effects (i.e., the influence of the second coordination shell) further enhance the positive charge on the C atoms. This effect is too small to be resolved and therefore is neglected.

It has been argued that the symmetry of the graphite rings is broken as nitrogen substitutes for a few of the nonbridgehead (i.e., perimeter) carbon atoms in the graphite microdomains of the films.[11] In this scenario, the comparison of the nitrogen-free and nitrogen-containing a-C:H films becomes analogous to the comparison of benzene (six carbon atoms in an aromatic ring) and pyridine (five carbons and one nitrogen atom in an aromatic ring).[11] We perform XPS measurements on pyridine and benzene films condensed on a sputter-cleaned Au substrate held at a temperature of 87 K. The condensation processes are performed in the analysis chamber at pyridine and benzene pressures of 3.0×10^{-7} mbar and 5.0×10^{-7} mbar, respectively. Thicknesses were optimized as discussed above.

Figure 4 shows a comparison of the C 1s XPS core-level spectra in a-C:H, a-CN_x:H ($x=0.1$), benzene, and pyridine. We measure the C 1s binding energy to be

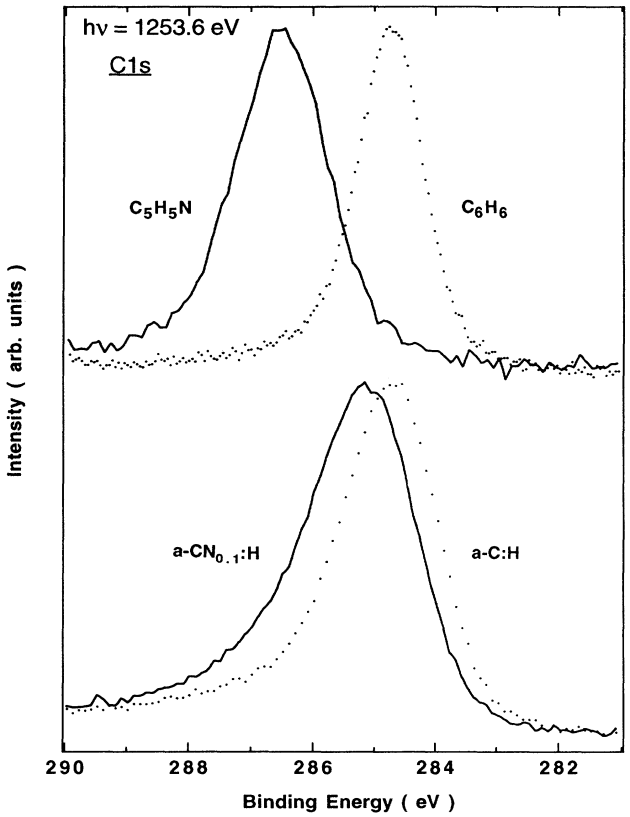

FIG. 4. XPS C 1s core-level spectra of ion-beam-deposited hydrogenated amorphous carbon a-C:H, nitrogen containing amorphous hydrogenated carbon a-CN_xH ($x=0.1$), and condensed pyridine C_5H_5N ($T=87$ K) and benzene C_6H_6 ($T=87$ K), measured with Mg $K\alpha$ radiation.

284.8 eV in benzene as opposed to 286.6 eV in pyridine, so that the chemical shift of the C 1s resulting from the replacement of one carbon atom by a nitrogen atom when going from benzene to pyridine is of the order of 1.8 eV. Note that there is no hydrogen attached to the nitrogen in pyridine; the lone pair of electrons on nitrogen is to be found in an orbital of approximately sp^2 hybridization lying in the plane of the ring, and belongs to the σ system. The 1.8-eV chemical shift when going from benzene to pyridine is substantially higher than the 0.4-eV value measured when going from a-C:H to a-CN_x:H ($x=0.1$). The C 1s FWHM's in benzene and pyridine are 1.25 and 1.74 eV, respectively. This 40% linewidth increase is higher than the 16% width increase corresponding to the 0.4-eV shift when going from a-C:H to a-CN_x:H ($x=0.1$). We account for the nitrogen concentration difference in a-CN_x:H ($x=0.1$) as compared to pyridine, (i.e., 9.0 at. % vs 16.7 at. %, respectively), by using the C 1s binding energies in benzene and pyridine, and assuming a linear dependence of the binding energy on the nitrogen content. This simple argument would place the C 1s binding energy in a-CN_x:H ($x=0.1$) about 0.6 eV higher than the observed 285.2 eV, and would correspond to a 1.0-eV chemical shift compared to a-C:H. This value would be 2.5 times higher than the observed 0.4-eV value.

Therefore, the relatively smaller chemical shift of the C 1s core level in a-CN_x:H ($x=0.1$), as compared to pyridine, cannot be explained on the basis of a lower nitrogen content alone.

The asymmetry of the line shape of the C 1s in a-CN_x:H ($x=0.1$) and the corresponding 16% linewidth increase, as compared to a-C:H, are suggestive of the existence of at least two phases. Therefore, we consider the C 1s core-level spectra within a two-phase mixture model. One phase corresponds to C atoms in an a-C:H environment surrounded by H and C atoms, and contributes to the low binding-energy region of the spectrum. The other phase, on the high binding-energy side, corresponds to C atoms in an a-CN_x:H environment surrounded by N, H, and C atoms. A least-squares fit of the data based on such a model, with the two different phases assumed to have Gaussian line shapes, is shown in Fig. 5. The effective C 1s binding energies in a-C:H and a-CN_x:H environments obtained from this exercise are 285.0 and 286.2 eV, respectively, a 1.2-eV effective chemical shift of the C 1s upon nitrogen incorporation. The effective concentration of C atoms in the a-CN_x:H phase is given by

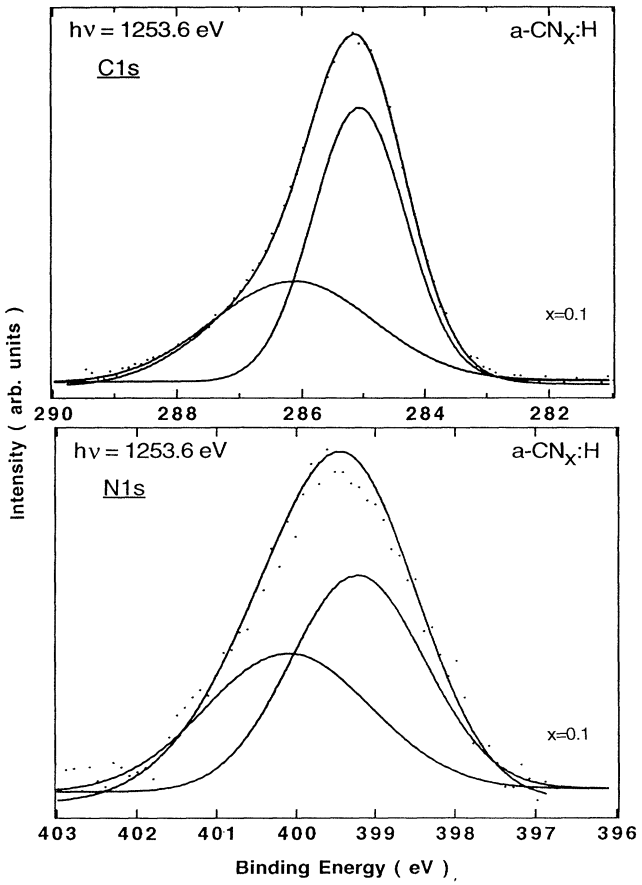

FIG. 5. C 1s and N 1s core-level spectra in a-CN_x:H for selected nitrogen concentrations x measured with Mg $K\alpha$ radiation. Dots are the measured data, and the solid line is the result of a least-squares fit based on a two-phase superimposition model as described in the text.

the empirical area ratio of the a-CN_x:H to a-C:H phases, and amounts to 38%.

As stated above, the $N1s$ binding energy and peak width remain constant for the entire range of nitrogen concentration in a-CN_x:H. In an ideal network structure of CN_x, nitrogen would always be fully coordinated by three carbon atoms. Under these ideal conditions, no chemical shift with changes in concentration would be expected. It is more realistic, however, to assume that the presence of hydrogen in the a-CN_x:H network is most likely to favor the creation of N-H bonds (in addition to the formation of C-N bonds). IR spectroscopy on samples prepared by plasma decomposition of a feedstock of CH_4 and N_2 in a capacitively coupled rf plasma reactor showed an increase of NH_2 and NC bonds with increasing N incorporation.[10] These results are interpreted in terms of an atomic structure consisting of a carbon backbone surrounded by a N coating, itself surrounded by a H coating.[10] The formation of N bonds with atoms less electronegative than C, such as H, increases the negative charge which resides on the N atoms and would induce, in principle, the formation of an asymmetric or weaker shoulder towards lower binding energies. The substantially larger width of the N 1s core level in a-CN_x:H ($x=0.1$), as compared to pyridine (2.3 vs 1.4 eV FWHM), and its lower binding energy (399.5 vs 400.5 eV) is consistent with a higher negative charge on the N atoms, i.e., the formation of N-H bonds in addition to N-C bonds. The abnormally large width of the N 1s level may be accounted for by assuming, as in the case of the C 1s core-level spectra, the existence of at least two phases: one with the N atoms surrounded by C atoms in an a-CN_x environment (the high binding-energy side of the spectrum) and the other with the N atoms in a NH_y environment surrounded by H atoms (the low binding-energy region of the spectrum). A least-squares fit decomposition assuming Gaussian-type line shapes for the two phases is shown in Fig. 5. The effective concentration of N atoms in a a-CN_x environment as given by the area ratio of the a-CN_x to NH_y phases is estimated to be 46%.

B. Plasmon losses

Complementary information on the electronic structure of the films is obtained from EELS measurements measured with 500-eV electron excitation. Figure 6 shows the EELS spectra for selected nitrogen concentrations in a-CN_x. The spectra are normalized to the same intensity of the 0-eV primary peak. The structure of the EELS spectra displays a dominant high-energy broad maximum around 25 eV and a much narrower peak around 6.0 eV. The 2.5-eV edge observed in the a-C:H EELS spectrum corresponds to loss features originating from the Au substrate, and superimposed onto those from the film. It is due to an interband transition from the Au 5d electrons into the conduction band. The 25-eV broad loss peak is considered to be responsible for the plasma oscillations of the entire ($\sigma+\pi$) valence-band electrons and is characteristic of bulk-plasmon losses.[18,19] The 6.0-eV loss peak is generally associated with the plas-

ma oscillations of the π electrons in graphitically bonded carbon atoms on sp^2 sites (π-type plasmon losses). In fact, it is more likely related to an antisymmetric mode ω in which the σ and π electrons are oscillating out of phase, with an amplitude dominated by the π oscillations.[20,21] No apparent energy shifts of the two characteristic energy-loss peaks are observed for different nitrogen concentrations in a-CN_x:H films. However, the relative intensity of the 6.0-eV π-type plasmon loss is found to increase slightly with increasing (x). The π plasmon provides a good qualitative fingerprint of the relative amount of graphitelike (sp^2) to diamondlike (sp^3) bonds. The observed evolution of its intensity as a function of nitrogen content is then suggestive of a small degree of graphitization upon nitrogen incorporation. Such an increase of the graphitic phase is shown below to be consistent with the changes observed in the π-related features of the valence band. The valence electron density (N_v) is related to the mass density (ρ) and the nitrogen content (x) according to

$$N_v=\rho(n_C+xn_N/A_C+xA_N)L_A ,$$

where L_A is Avogadro's number, A_C (=12) and A_N (=14) the atomic weights of C and N, respectively, and n_C (=4) and n_N (=5) the number of valence electrons of C and N, respectively.

Assuming the free-electron approximation to be valid,[22] a valence electron density N_v of 4.5×10^{23} e^-/cm^3 is derived from the observed energy of the ($\sigma+\pi$) bulk-plasmon loss peak. The sample density (ρ) thus obtained using the experimentally determined plasmon energy is 2.2 ± 0.2 g/cm^3. This value coincides with the upper limit of the accepted range of values of hard a-C:H ($1.6<\rho<2.2$ g/cm^3), as opposed to soft polymerlike a-C:H with density values ranging from 0.9 to 1.6 g/cm^3.[23] It indicates that the films have retained, upon nitrogen incorporation, the basic physical characteristics of amorphous hard carbon.

C. Valence-band spectra

Figure 7 shows the UPS valence-band spectra of our various films measured with 21.2 and 40.8 eV excitation energies, corresponding to He I and He II radiations, respectively. The spectra have been corrected for excitation by UV satellites above the main line. The angle integrated UPS valence-band spectra of amorphous materials can be interpreted in the density-of-states (DOS) picture, and reveal essentially a sum of partial density of states, weighted with the corresponding photoionization cross sections.[24] The photoionization cross section for C 2s and C 2p electron states is strongly dependent on the excitation energy; atomic photoionization cross-section calculations for C 2s and C 2p electron states at a photon energy of 21.2 eV are 1.2 ad 6.1 Mb, respectively. The corresponding values at 40.8-eV photon energy are 1.2 and 1.9 Mb, respectively.[25] Therefore, the low photon-energy UPS spectra of our a-CN_x:H films are dominated by the 2p electron states and will be interpreted mainly in terms of the partial p-DOS. The measured density of states recorded at the two different excitation energies are essentially similar in the low binding-energy region (see Fig. 7). They exhibit a very smooth shape, typical of

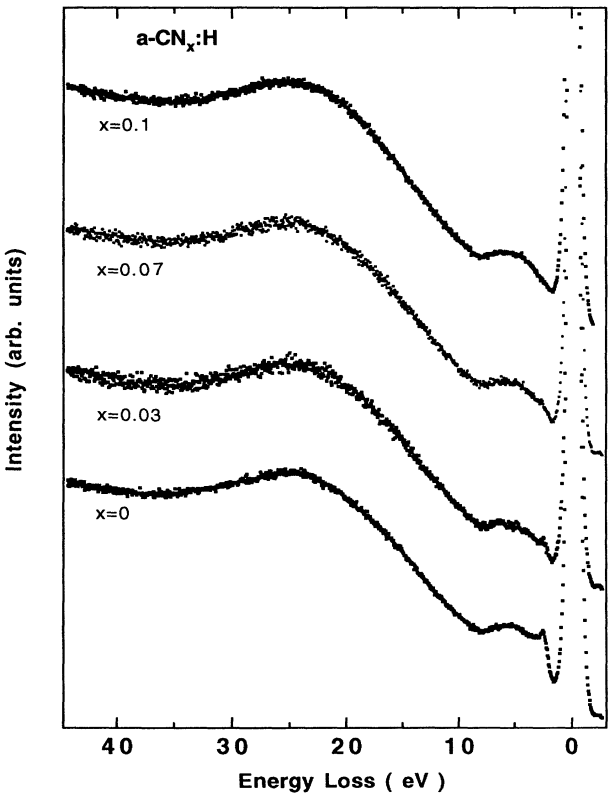

FIG. 6. EELS spectra of a-CN_x:H measured with 500-eV primary electrons. The spectra are normalized to the same intensity height of the 0-eV primary peak.

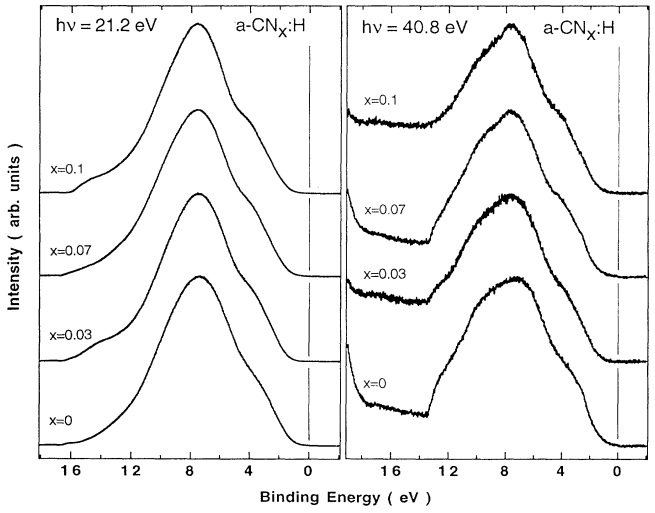

FIG. 7. UPS He I ($h\nu$=21.2 eV) and He II ($h\nu$=40.8 eV) valence-band spectra of a-CN_x:H. The zero of energy is the Fermi level. The spectra have been corrected for UV satellites above the Fermi energy.

amorphous materials, and display basically a prominent peak at about 7 eV, and a leading shoulder at the top of the valence band near 4 eV. The 7- and 4-eV features, similar to those observed in the soft-x-ray-emission spectra of graphite,[26] and alkali-intercalated graphite compounds,[27] are related to the p-σ and p-π contributions to the DOS, respectively. The shoulder at 4 eV has been reported already to be present in He I valence-band spectra of a-C:H films prepared under similar conditions,[15] but was not visible in the 120-eV photoemission spectra of a-C:H films produced by dc glow discharge of ethylene.[28] The π contribution becomes apparent only upon annealing, as hydrogen is evolving from the films and the films become more graphitic in nature. The hint of a kink of 13 eV in the He II spectrum of a-C:H is reminiscent of the 13-eV peak of mixed s and p character present in graphite[19] and in diamond.[29] It is virtually suppressed in the corresponding He I spectrum because of the higher photoionization cross section of the C($2p$) orbital relative to the C($2s$) at that excitation photon energy.[25]

In discussing the influence of nitrogen on the shape of the He I valence-band spectra, let us first point out the importance of the background at inelastically scattered electrons in the higher binding-energy region of He I valence-band spectra. Caution must be exercised in interpreting changes observed in the high binding-energy region of the spectra on incorporation of nitrogen. Then there are three features of note in the changes observed in the He I valence-band spectra upon nitrogen incorporation.

First, the position of the valence-band maximum E_{VBM}, determined by the extrapolation of the steepest descent of the leading edge of the spectrum to the base line, is found to increase linearly relative to the Fermi level from 1.11 eV in a-C:H up with increasing x to 1.45 eV in a-CN_x:H ($x=0.1$). For reasons mentioned above, this increase is not to be attributed to charging effects. The variation of E_F-E_{VBM} as a function of x is depicted in Fig. 8(a). This gradual increase of E_F-E_{VBM} with x can be interpreted either in terms of a recession of the VBM with respect to a fixed Fermi level, or in terms of shifts of E_F within the forbidden gap. In order to distinguish between these two mechanisms, a tentative energy-level diagram is proposed in Fig. 8(b), where the VBM and E_F are plotted relative to the N 1s core level, which did not undergo any chemical shifts. Also included is the position of the conduction-band minimum E_{CBM}, obtained by adding to our measured VBM energies the optical gap E_g [measured on samples prepared by rf plasma using a feedstock of CH_4 and N_2 (Ref. 10)]. From Fig. 8, the VBM is seen to recede rapidly by 0.3 eV for low nitrogen content ($x<0.03$) before becoming largely independent of the nitrogen level on addition of more nitrogen ($x>0.03$). Despite the considerable uncertainty in determining the position of the CBM, since the optical gap and the VBM have not been measured on the same samples, the CBM is clearly moving downward with x towards a fixed E_F. It starts within 1.4 eV from E_F in a-C:H, reaches a position within 1.1 eV from E_F for $x=0.03$, before ending within 0.9 eV from E_F for $x=0.1$, in a way as to bring the Fermi-level position

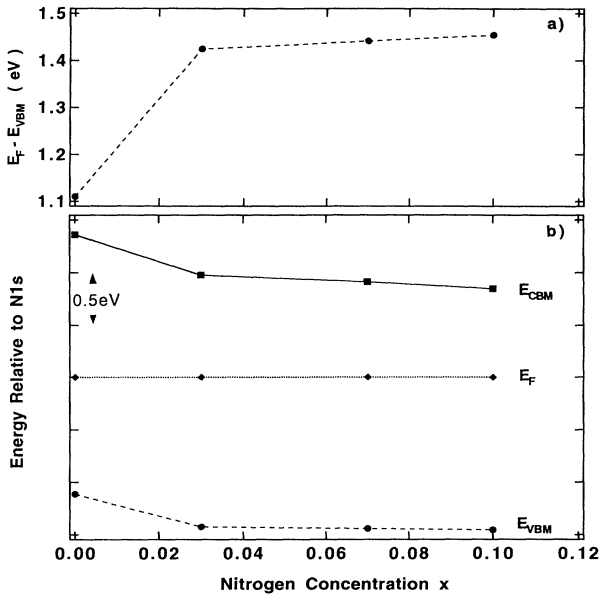

FIG. 8. (a) Position of E_F relative to the VBM in a-CN_x:H as a function of nitrogen concentration x. (b) Position of the VBM and E_F relative to the N 1s core level as a function of nitrogen concentration x. The position of the CBM is obtained by adding to our measured VBM values the optical gap of rf a-CN_x:H samples from Ref. 10.

from a midgap position in a-C:H to a position above the midgap in a-CN_x:H, but still in the conduction tail, below the conduction-band edge. It is interesting to note the basically similar behavior of the VBM and CBM with respect to the Fermi level. A 0.3-eV downward shift with respect to E_F is deduced in both cases for low nitrogen content ($x<0.03$). The VBM does not shift any further at higher levels of nitrogen, while the CBM moves downward by a mere 0.2 eV for $0.03<x<0.1$. The decreasing (relative) separation between E_F and CBM as a function of the nitrogen concentration can be correlated with a decrease in the activation energy.[5]

A second point of note is the gradual washing out of the 13-eV kink as the nitrogen level in the film increases (Fig. 7). The absence of this peak in the a-C:H valence-band spectrum has been discussed in terms of odd-membered rings in the random network of a-C:H, which are favored by the predominently sp^3 coordinated carbon atoms.[7,8] We interpret this behavior as an increase of the fraction of sp^2 coordinated sites for nitrogen-containing a-CN_x:H films. This in accordance with the graphitization process evidenced by the intensity increase of the π plasmon in the above EELS spectra.

Thirdly, in spite of the favorable photoionization cross section of the nitrogen $2p$ orbital as compared to the carbon $2p$ orbital (9.7 vs 6.1 Mb at 21.2-eV excitation energy, and 4.4 vs 1.9 Mb at 40.8 eV, respectively),[25] there are no obvious nitrogen-related features in the valence band of a-CN_x:H films.

In order to probe the finer details of the effects of nitrogen incorporation on the spectral shape of the DOS, we propose to fit the He I valence-band spectrum with a sim-

ple model consisting of a combination of two single line-shape functions. We assume, to a first approximation, Gaussian line-shape functions to account for the broadening of the states. We argue that the Gaussian parameters, the width in particular, reflect the changes in the DOS upon nitrogen incorporation. Because of their weaker bonding character, and their delocalized nature, the graphitelike π bonds at sp^2 sites are responsible for dominating the electronic properties of a-C:H, whereas the mechanical properties are governed by the σ bonds.[7,8] Therefore we expect the effects of nitrogen on the DOS spectral shape to be reflected more predominantly in the variation of the partial p-π DOS, and to be only minor in the p-σ part of the valence-band DOS.

We restrict the fitting range of the He I valence-band spectra to the 0.9-eV region because of the uncertainty on the band shapes in the high binding-energy region: As stated above, the background of inelastically scattered electrons may cause distortions of the band line shape in that energy region. Figure 9 shows the result of our model fitted to the He I valence-band spectra of a-C:H and a-CN_x:H ($x=0.1$). The parameters of the model fitted to the a-CN_x:H films valence-band spectra with different nitrogen concentrations are shown in Table I.

As expected, these results illustrate how sensitive the

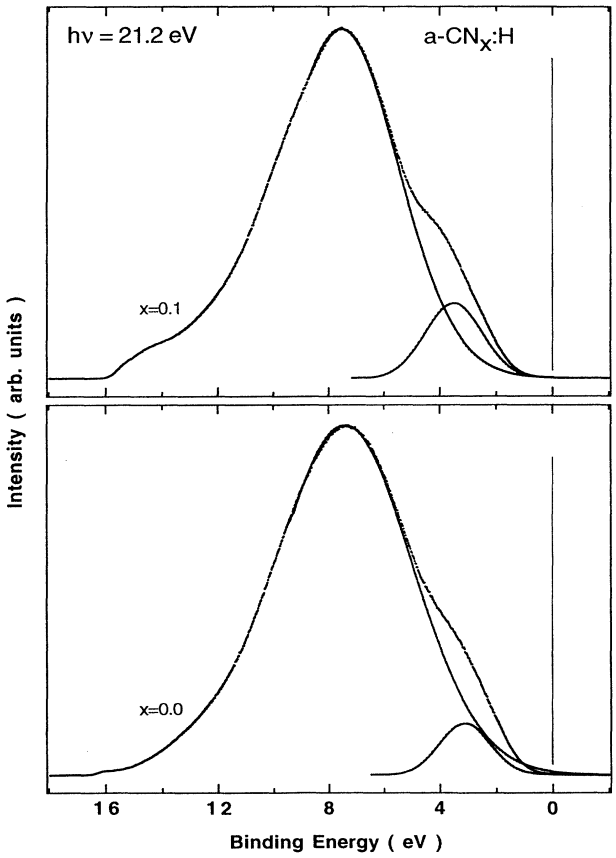

FIG. 9. UPS He I ($h\nu=21.2$ eV) valence-band spectra of a-C:H and a-CN_x:H films (dotted lines), and a deconvolution fit (solid lines) revealing the partial p-σ and p-π density of states (DOS) as described in the text.

TABLE I. Parameters of the two-Gaussian fit to the He I ($h\nu=21.2$ eV) valence-band spectra of a-CN_x:H. x is the nitrogen concentration. E_σ and E_π are the positions of the partial p-σ and p-π parts of the valence band, respectively, Γ_π is the FWHM of the p-π corresponding Gaussian broadening function. A_R is the area ratio of the p-π to p-σ contributions to the valence band between 0 and 9 eV. E_F-E_{VBM} is the position relative to E_F of the VBM, obtained as described in the text.

Nitrogen content x	E_σ (eV)	E_π (eV)	Γ_π (eV)	A_R	E_F-E_{VBM} (eV)
0	7.44	3.16	2.1	0.05	1.11
0.03	7.51	3.42	2.14	0.07	1.42
0.07	7.61	3.5	2.21	0.07	1.44
0.1	7.61	3.58	2.41	0.11	1.45

p-π part of the valence band is to the presence of nitrogen, while the p-σ part is only weakly dependent on the nitrogen content. In particular, it is found that the width Γ_π of the π contribution at the top of the valence band increases as the nitrogen content in the film increases. Similarly, its area relative to that of the σ contribution increases with increasing x, and indicates that the films have retained the basic physical characteristics of amorphous hard carbon; a decrease of the p-π related shoulder has been shown to be the ansatz of a polymeric structure of a-C:H, as compared to hard a-C:H.[30]

According to Robertson and O'Reilly,[7,8] the π states on sp^2 sites tend to cluster together in aromatic rings, forming graphitic islands, and the width of the peaks in the DOS corresponding to π states is correlated to the distribution of island sizes. Within this model, our experimentally determined increase in width and relative area of the p-π DOS on increased nitrogen content implies larger π bonded clusters, and larger defect density. The merging with the valence-band tail of these higher density gap states has resulted in the extension of the band tails. This may explain why the VBM position (with respect to E_F) recedes at low nitrogen levels ($x<0.03$), and then remains unaffected at higher nitrogen contents ($x>0.03$). For low nitrogen content, downward shifts of both the CBM and VBM are observed. The downward shift of the CBM towards a fixed E_F and the relatively unaffected position of the VBM with respect to the Fermi level for high nitrogen content may both suggest a conductivity enhancement caused by additional localized states which move the conduction band closer to E_F.[5]

IV. CONCLUSION

We have prepared nitrogen containing hydrogenated amorphous carbon films with different nitrogen contents by ion-beam deposition. The nitrogen incorporation is found to induce graphitization as evidenced by a slight increase in the π characteristic energy loss in the EELS spectra and by the increase in the p-π contribution to the He I valence density of states. The higher p-π contribution to the valence band in the nitrogen-containing films, and their high density deduced from the EELS measurements indicate that the films have retained the basic physical characteristics of amorphous hard carbon.

Photoemission measurements reveal binding-energy shifts of the C 1s core-level spectra as a function of nitrogen content. We do not attribute these shifts to a shift of the Fermi level with respect to the top of the valence band, as would be expected from a substitutional doping mechanism. We identify these shifts as chemical in nature. Measurements performed on model compounds, pyridine and benzene, enable us to explain the variation of the line shape and peak position of C 1s core level in terms of a model containing two phases, a-CN_x:H and a-C:H. Similarly, we interpret the N 1s core-level line shape and peak position in terms of a two-phase mixture of a-CN_x and NH_y phases.

A simple model fit to the He I UPS valence-band spectra reveals the effects of nitrogen on the spectral shape of the DOS, in particular, the sensitivity of the p-π DOS to the presence of nitrogen. It confirms the role played by the π bonds in controlling the electronic structure of a-C:H. The increases in area and width of the p-π DOS with increasing nitrogen content are in line with an existing model that describes increases in both defect density and size of the graphitic islands formed by the clustering of π states in aromatic rings. The subsequent extension of the band tails may explain why the VBM position (with respect to E_F) becomes largely independent of the nitrogen concentration contents, whereas low nitrogen incorporation is found to induce a downward shift of both the VBM and CBM positions.

ACKNOWLEDGMENTS

This work has been carried out in the Electron Spectroscopy Laboratory of Professor Peter Oelhafen, whom we wish to thank for enlightening discussions. We wish to thank Dr. Jane Frommer for her careful reading of the manuscript. The financial support of the Swiss National Science Fundation is gratefully acknowledged.

*Present address: Habasit AG, Römerstrasse 1, Reinach-Basel, CH-4153, Switzerland.

[1]J. C. Angus, P. Koidl, and S. Domitz, in *Plasma Deposited Thun Films,* edited by J. Mort and F. Jansen (CRC, Boca Raton, FL, 1986), p. 89.

[2]J. C. Angus and C. C. Hayman, Science **241**, 913 (1988).

[3]*Amorphous Hydrogenated Carbon Films, E-MRS Symp. Proc. Vol. XVII,* edited by P. Koidl and P. Oelhafen (Les Editions de Physique, Les Ulis, 1987).

[4]B. Meyerson and F. W. Smith, Solid State Commun. **34**, 531 (1980).

[5]D. I. Jones and A. D. Stewart, Philos. Mag. B **46**, 423 (1982).

[6]O. Amir and R. Kalish, J. Appl. Phys. **70**, 4958 (1991).

[7]J. Robertson, Adv. Phys. **35**, 317 (1986).

[8]J. Robertson and E. P. O'Reilly, Phys. Rev. B **35**, 2946 (1987).

[9]B. Dunnett, D. I. Jones, and A. D. Stewart, Philos. Mag. B **53**, 159 (1986).

[10]H.-X. Han and B. J. Feldman, Solid State Commun. **65**, 921 (1988).

[11]J. H. Kaufman, S. Metin, and D. D. Saperstein, Phys. Rev. B **39**, 13 053 (1989).

[12]S. Lin, Kevin Noonan, Bernard J. Feldman, Dong Min, and M. T. Jones, Solid State Commun. **80**, 101 (1991).

[13]H. R. Kaufman, J. Vac. Sci. Technol. **15**, 272 (1978).

[14]D. Ugolini, M.-H. Tuilier, J. Eitle, S. Schelz, J. Q. Wang, and P. Oelhafen, Appl. Phys. A **51**, 526 (1990).

[15]D. Ugolini, P. Oelhafen, and M. Wittmer, in *Amorphous Hydrogenated Carbon Films,* edited by P. Koidl and P. Oelhafen (Les Editions de Physique, Les Ulis, France, 1987), p. 297.

[16]J. Scofield, J. Electron Spectros. Relat. Phenom. **8**, 129 (1976).

[17]L. Pauling, *The Nature of Chemical Bonds,* 3rd ed. (Cornell University Press, New York, 1960).

[18]H. Venghaus, Phys. Status, Solidi B **71**, 609 (1975).

[19]F. R. McFeely, S. P. Kowalczykk, L. Ley, R. G. Cavell, R. A. Pollack, and D. A. Shirley, Phys. Rev. B **9**, 5268 (1974).

[20]H. Raether, *Excitation of Plasmons and Interband Transitions by Electrons,* edited by G. Höhler, Springer Tracts in Modern Physics Vol. 88 (Springer-Verlag, Berlin 1980).

[21]H. Cohen, E. Kolodney, T. Maniv, and M. Folman, Solid State Commun. **81**, 183 (1992).

[22]P. M. Platzman and P. A. Wolff, in *Waves and Interactions in Solid State Plasma* (Academic, New York, 1973).

[23]P. Koidl, C. Wild, B. Dischler, J. Wagner, and M. Ramsteiner, Mater. Sci. Forum **52**, 41 (1989).

[24]P. Oelhafen, in *Amorphous and Liquid Material,* Vol. 118 of *NATO Advance Study Institute Series E: Applied Sciences,* edited by E. Luscher, G. Fritsch, and G. Jacucci, (Martinus Nijhoff, Dordrecht, 1987).

[25]J. J. Yeh and I. Lindau, At. Data Nucl. Data Tables **32**, 1 (1985).

[26]A. Mansour, R. D. Carson, and S. E. Schnatterly, Phys. Rev. B **31**, 6521 (1985).

[27]A. Mansour and S. E. Schnatterly, Phys. Rev. Lett. **58**, 614 (1987).

[28]D. Wesner *et al.*, Phys. Rev. B **28**, 2152 (1983).

[29]A. Mansour, G. Indlekofer, and P. Oelhafen, Appl. Surf. Sci. **48/49**, 312 (1991).

[30]D. Ugolini, J. Eitle, and P. Oelhafen, Vacuum **41**, 1374 (1990).